CORA Cork Open Research Archive
Cartlann Taighde Oscailte Chorcaí

Title	First-principles calculation of carrier-phonon scattering in n-type Si1–xGex alloys
Authors	Murphy-Armando, Felipe;Fahy, Stephen B.
Publication date	2008-07-01
Original Citation	MURPHY-ARMANDO, F. & FAHY, S. B. 2008. 'First-principles calculation of carrier-phonon scattering in n-type Si1–xGex alloys'. Physical Review B, 78, 035202. doi:10.1103/PhysRevB.78.035202
Type of publication	Article (peer-reviewed)
Link to publisher's version	http://link.aps.org/doi/10.1103/PhysRevB.78.035202 - 10.1103/PhysRevB.78.035202
Rights	©2008 The American Physical Society
Download date	2026-11-07 20:15:27
Item downloaded from	https://hdl.handle.net/10468/2673

UCC
University College Cork, Ireland
Coláiste na hOllscoile Corcaigh

First-principles calculation of carrier-phonon scattering in *n*-type $Si_{1-x}Ge_x$ alloys

F. Murphy-Armando and S. Fahy
Department of Physics and Tyndall National Institute, University College Cork, Cork, Ireland
(Received 30 January 2008; revised manuscript received 29 April 2008; published 3 July 2008)

First-principles electronic structure methods are used to find the rates of inelastic intravalley and intervalley *n*-type carrier scattering in $Si_{1-x}Ge_x$ alloys. Scattering parameters for all relevant Δ and *L* intra- and intervalley scattering are calculated. The short-wavelength acoustic and the optical phonon modes in the alloy are computed using the random mass approximation, with interatomic forces calculated in the virtual crystal approximation using density functional perturbation theory. Optical phonon and intervalley scattering matrix elements are calculated from these modes of the disordered alloy. It is found that alloy disorder has only a small effect on the overall inelastic intervalley scattering rate at room temperature. Intravalley acoustic scattering rates are calculated within the deformation potential approximation. The acoustic deformation potentials are found directly and the range of validity of the deformation potential approximation verified in long-wavelength frozen phonon calculations. Details of the calculation of elastic alloy scattering rates presented in an earlier paper are also given. Elastic alloy disorder scattering is found to dominate over inelastic scattering, except for almost pure silicon ($x \approx 0$) or almost pure germanium ($x \approx 1$), where acoustic phonon scattering is predominant. The *n*-type carrier mobility, calculated from the total (elastic plus inelastic) scattering rate, using the Boltzmann transport equation in the relaxation time approximation, is in excellent agreement with experiments on bulk, unstrained alloys.

DOI: 10.1103/PhysRevB.78.035202 PACS number(s): 72.80.Cw, 71.55.Cn, 72.10.−d, 72.80.Ng

I. INTRODUCTION

SiGe has been studied for many years as an ideal, prototypical, binary semiconductor alloy.[1] Recently, its use in complementary metal-oxide semiconductor (CMOS) technology has increased due to its versatility in heterostructure devices, where transport properties are of key importance.[2] As alloying, strain engineering and quantum confinement change the electronic states and their coupling to the chemical or vibrational fluctuations in the active region of a device, different physical mechanisms of the carrier scattering (e.g., alloy disorder, interface roughness, intervalley or intravalley phonon scattering) may increase or decrease in importance. While carrier mobility measurements in bulk systems provide much information about scattering mechanisms, they do not always uniquely determine the separate contributions.[1] Thus, it is of considerable practical and physical interest to be able to theoretically predict the charge transport properties of semiconductor devices from a knowledge of their atomic structure only. Ideally, we would like to be able to do so with a level of quantitative confidence comparable to that with which we can now calculate structural and vibrational properties of atomic-scale structures.

Our aim in this paper is to present general, first-principles electronic structure theory methods, by which carrier mobility can be calculated from a knowledge of atomic-scale structure only, without phenomenological input. We will restrict our applications here to those required to give a complete, first-principles calculation of carrier scattering in bulk SiGe alloys, but we expect that some of the techniques and scattering parameters for the SiGe system will be applicable, with some modification, in other contexts. In particular, the scattering parameters and deformation potentials may be of interest in the study of transport in devices.

Theoretical work on elastic carrier scattering due to disorder in binary alloys has advanced greatly since the early work of Nordheim.[3] A notable example of these methods is the coherent potential approximation, or CPA, in which the scattering rates are calculated in terms of the scattering by individual alloy constituents.[4,5] By and large, these developments have treated the interaction of individual atoms with the carrier states on a phenomenological basis.

The earliest theoretical study of the electronic transport properties of pure silicon or germanium concentrated on inelastic scattering by acoustic phonons, using measured or phenomenological values of the acoustic deformation potentials.[6] *Ab initio* calculations of physical properties, such as the acoustic[7,8] and intervalley[9] deformation potentials, required to find the carrier scattering, have been previously performed for Si and Ge, albeit using a model solid approach or with the Harris functional. The first work[10] to calculate transport properties from *ab initio* electronic structure theory obtained the elastic alloy scattering in SiGe, and included inelastic phonon scattering phenomenologically. Subsequently, this approach was also applied to find the hole mobility in SiGe[11] and carrier mobilities in GeSn.[12] More recently,[13] a full *ab initio* method has been applied to obtain electron-phonon relaxation times in GaAs and GaP. Earlier calculations performed with empirical methods[1,14–16] had to rely on often inaccurate experimental data, and were unable to determine the relative strength of the different scattering mechanisms.

Before the work of Ref. 10, alloy intervalley scattering had either been deemed negligible,[1] or could not be distinguished from intravalley scattering.[14,16–19] The relative strength of intra- and intervalley scattering is of particular importance in understanding mobility in strained SiGe alloys because strain lifts the degeneracy of the valleys and removes certain scattering channels (in particular, intervalley *f*-type scattering in Si-rich alloys and *L*-*L* scattering in Ge-rich alloys), which are available in the cubic system.

 ©2008 The American Physical Society

In this paper we calculate from first principles the *n*-type carrier scattering by phonons in an ideal, perfectly random SiGe alloy. To give a complete treatment of the carrier scattering in this system, we also present full details of the first-principles calculation of elastic alloy scattering, first given briefly in Ref. 10. Together, these provide a complete first-principles description of *n*-type carrier scattering in this alloy, which is in excellent agreement with available experimental data. The methods outlined here are not specialized for SiGe, but can readily be used to calculate carrier mobility for a range of conventional strained or unstrained semiconductor alloys.

An important contribution of this paper is the set of calculated parameters governing transport, which may be used in further phenomenological calculations. Readers interested in using these parameters should concentrate on Secs. VII A 2 and VII A 3, in which the value of the calculated intra- and intervalley electron-phonon coupling parameters, respectively, are presented. The remaining sections describe the method for calculating the parameters from first-principles electronic structure theory.

In Sec. II, we review the relevant aspects of the conduction bands of SiGe alloys and their calculation, using density functional theory (DFT) and the more accurate GW quasiparticle theory.[20] We then derive in Sec. III a general expression[10] for elastic alloy scattering in a weakly-scattering binary alloy, which is suitable for use in the context of first-principles supercell electronic structure methods. While it is well known that the DFT band structure does not necessarily reproduce the correct quasiparticle band structure that is relevant for carrier dynamics, nevertheless the largest error typically occurs in the band gap, rather than in the conduction or valence band dispersions. For Si and Ge, the DFT conduction-band dispersions and pressure dependence of the band gap are generally in good agreement with experiment.[21,22] Indeed, this is the basis for using the DFT approach to calculate the carrier scattering and an important outcome from this work is the demonstration that the results obtained for mobility in SiGe alloys are in good agreement with experiment.

Inelastic scattering of carriers by phonons is discussed in Sec. IV. We divide the inelastic phonon-scattering problem into two different regimes: (a) scattering by optical and short-wavelength acoustic phonons, where the phonon wavelength is comparable to the interatomic distance and alloy disorder is expected to strongly affect the phonon spectrum,[23] and (b) scattering by acoustic phonons, where the phonon wavelength is long compared to the variation in the random alloy potential. We find that interatomic forces and the coupling of atomic displacements to the electronic states can be well treated in either regime within the virtual crystal approximation (VCA).

The first regime requires the simulation of a sufficiently large region of random alloy (several hundred atoms) to accurately represent the various bonding arrangements between Si and Ge atoms, which affect the high-frequency phonon spectrum. We find that the random mass approximation represents the phonon spectra and the electron-phonon coupling well in this high-frequency regime. These phonons govern the inelastic intervalley carrier scattering, as well as optical intravalley scattering.

In the second regime, the long-wavelength phonons are well represented in the average mass approximation, where all atomic masses are replaced by the average atomic mass, and the electron-phonon interaction is treated within the deformation potential approximation. These phonons have short wave vectors and low frequencies and give rise to quasielastic intravalley scattering. We use a frozen phonon supercell approach to calculate the deformation potentials for long-wavelength acoustic phonons, which allows us to obtain their wave vector dependence and demonstrate that the deformation potential approximation is accurate in treating intravalley acoustic scattering.

In Sec. V we give an expression for the total carrier mobility, calculated using the Boltzmann transport equation in the relaxation time approximation.

In Secs. VI and VII of the paper, we apply these methods to random SiGe alloys and calculate the parameters determining the inelastic intravalley Δ and L scattering, f- and g-type Δ intervalley scattering, and L intra- and intervalley scattering. We present the acoustic, optical and intervalley deformation potentials, and compare them, where available, to previous theoretical and experimental results. Elastic alloy scattering parameters have been given in Ref. 10. We then calculate the *n*-type carrier scattering rate and find the carrier mobility.

Elastic alloy disorder scattering dominates over phonon scattering, except for almost pure silicon ($x \approx 0$) or almost pure germanium ($x \approx 1$). On the other hand, we find that considering alloy disorder explicitly in the calculation of the intervalley and optical phonon scattering makes very little difference, compared to an average mass treatment, in which alloy disorder is completely ignored.

II. CONDUCTION BAND MINIMA IN SiGe

Depending on alloy composition, the conduction band minimum in $Si_{1-x}Ge_x$ is either at the L-point or the Δ-point, $\mathbf{k}=\frac{2\pi}{a_0}(\xi,0,0)$, with $\xi=0.83$; if the alloy contains less than 85% Ge, the conduction band minimum is at the Δ valley, otherwise it is at the L valley. Near Ge content $x \approx 0.85$, scattering between the nearly degenerate Δ and L valleys becomes important. The Δ band has six equivalent valleys in the [001], [00$\bar{1}$], [010], [0$\bar{1}$0], [100], and [$\bar{1}$00] crystallographic directions, while the L band has four equivalent valleys along the [111], [$\bar{1}$11], [1$\bar{1}$1], and [11$\bar{1}$] directions (see Fig. 1). Two distinct parameters characterize Δ intervalley scattering: [001]$\rightarrow$[00$\bar{1}$] is g-type and [001]$\rightarrow$[100] is f-type. The intervalley scattering between the L valleys requires only one parameter, which we shall label LL. The conduction bands in the Δ and L valleys display a quadratic dispersion in $\mathbf{k}$-vector near the band minimum at $\mathbf{k}_\alpha$:

$$E(\mathbf{k}) = E(\mathbf{k}_\alpha) + \frac{\hbar^2 \Delta k_\parallel^2}{2m_l^\alpha} + \frac{\hbar^2 \Delta k_\perp^2}{2m_t^\alpha}, \tag{1}$$

where $\Delta k_\parallel$ and $\Delta k_\perp$ are the components of $\mathbf{k}$-$\mathbf{k}_\alpha$ parallel and perpendicular, respectively, to $\mathbf{k}_\alpha$. The surfaces of constant energy are ellipsoids of revolution, with the axis of revolution parallel to the direction of the valley, $\mathbf{k}_\alpha$, as shown in

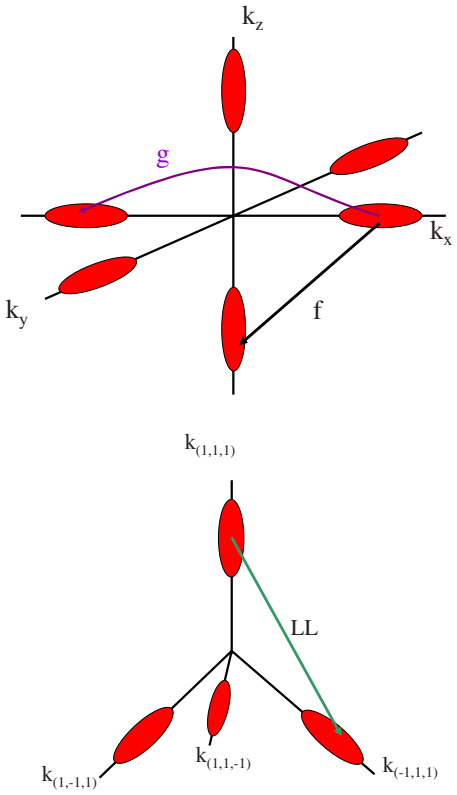


FIG. 1. (Color online) The surfaces of constant energy in the Δ valleys (upper panel) and L valleys (lower panel) for SiGe alloys. The intervalley f-type and intervalley g-type scattering matrix elements are indicated by lines between the Δ valleys, and the intervalley LL scattering matrix elements by a line between two of the L valleys.

Fig. 1. We can consider the carriers in valley α as free electrons with different effective masses, m_l^α or m_t^α, depending on the direction of motion: the longitudinal mass m_l for transport along the longitudinal axis direction, $\mathbf{k}_\alpha$, and the transverse mass m_t for transport along the transverse axes perpendicular to $\mathbf{k}_\alpha$.

Calculated and experimental values of the effective masses are shown in Table I (details of the calculations are given below). Also shown are the calculated values of the lattice constants and energy differences between important symmetry points. The agreement generally between calculated and measured values is excellent, except for the values of the band gap E_g.

Throughout this work we have used the VCA for the calculation of various properties of the average alloy. In this approximation, the ionic potential of an alloy atom at Ge composition x is built from the average of the ionic potentials of the alloy constituents, as

$$V_x^{\mathrm{VCA}} = xV^{\mathrm{Ge}} + (1-x)V^{\mathrm{Si}}. \tag{2}$$

The VCA proves very useful whenever the properties calculated do not depend strongly on alloy disorder.

III. ELASTIC ALLOY SCATTERING

In this section we derive an expression for the alloy scattering rate from Fermi's second golden rule and the T-matrix formalism.[25] If we consider two ideal crystal states, $\psi_{\mathbf{k}}$ and $\psi_{\mathbf{k}'}$ of equal energy, the scattering rate between them will be proportional to the T-matrix element squared, $|\langle\psi_{\mathbf{k}'}|T|\psi_{\mathbf{k}}\rangle|^2 = |\langle\psi_{\mathbf{k}'}|\Delta V|\phi_{\mathbf{k}}\rangle|^2$, where ΔV is the perturbing potential due to the deviations of the actual alloy potential from the average, perfectly periodic potential, and $\phi_{\mathbf{k}}$ is the eigenstate of the Hamiltonian with ΔV present. Thus, the elastic scattering rate at valley α for the alloy becomes

$$R(E(\mathbf{k}_\alpha)) = \frac{2\pi}{\hbar}\Omega\sum_\beta \int \frac{d^3k'_\beta}{(2\pi)^3}|\langle\psi_{\mathbf{k}'_\beta}|T|\psi_{\mathbf{k}_\alpha}\rangle|^2 \times \delta(E(\mathbf{k}_\alpha) - E(\mathbf{k}'_\beta)), \tag{3}$$

where Ω is the volume of the system, and β labels the valley into which scattering occurs. We now wish to find the dependence of Eq. (3) on the alloy composition. SiGe can be seen as a random substitutional alloy with two building blocks: one corresponding to Ge sites, with probability x, and one to Si sites, with probability $(1-x)$. We will make three assumptions about the alloy, which we shall test later: (i) that Si and Ge are relatively weak scatterers in the alloy, thus allowing us to consider that each site scatters the carriers independently; (ii) that the alloy is completely random, and there is no correlation between the atomic species on different sites; and (iii) that the average of the scattering matrix $\bar{T}(\mathbf{k},\mathbf{k}') = 0$. The last assumption is equivalent to the CPA,[4,5] where the average crystal does not scatter.

TABLE I. Calculated and experimental properties of Si and Ge used in this work. m_e is the free mass of the electron. All calculated properties were computed from DFT bands, using the LDA, except for $\Delta E_{\Delta L}$, where we used the GW quasiparticle method. The calculated value of $\Delta E_{\Delta L}$ is given as a function of alloy composition x and has been calculated within the VCA. Experimental values are from Ref. 24, except where noted.

Quantity	Units	Calculated	Exp.
m_l^Δ(Si)	m_e	0.95	(0.98 ± 0.04)
m_t^Δ(Si)	m_e	0.19	(0.19 ± 0.01)
m_l^L(Si)	m_e	1.89	
m_t^L(Si)	m_e	0.13	
$m_l^\Delta(\Delta_{\mathrm{Ge}})$	m_e	0.91	
$m_t^\Delta(\Delta_{\mathrm{Ge}})$	m_e	0.19	
m_l^L(Ge)	m_e	1.68	(1.64 ± 0.03)
m_t^L(Ge)	m_e	0.0816	(0.0819 ± 0.0003)
a_0(Si)	Bohr	10.1723	10.26
a_0(Ge)	Bohr	10.5503	10.69
E_g(Si)	eV	0.46	1.17[a]
E_g(Ge)	eV	0.23	0.744[a]
$\Gamma_{15c}\rightarrow X_{1c}$(Si)	eV	−1.98	−2.1 [a]
$\Gamma_{15c}\rightarrow L_{1c}$(Si)	eV	−1.06	−1.3,−1 [a]
$\Gamma_{7c}\rightarrow X_{5c}$(Ge)	eV	0.37	0.41[a]
$\Gamma_{7c}\rightarrow L_{1c}$(Ge)	eV	−0.048	−0.146 [a]
$\Delta E_{\Delta L}$	eV	$0.16(x-0.87)(x+7.32)$	

[a]Reference 20 and references therein.

The scattering amplitude for each site i is given by

$$T_i(\mathbf{k},\mathbf{k}') = \langle \psi_{\mathbf{k}}|T_i|\psi_{\mathbf{k}'}\rangle = \langle \psi_{\mathbf{k}}|V_i|\phi_{\mathbf{k}'}\rangle, \tag{4}$$

where V_i is the change in potential due to an impurity at site i. The total scattering amplitude is thus,

$$T(\mathbf{k},\mathbf{k}') = \langle \psi_{\mathbf{k}}|T|\psi_{\mathbf{k}'}\rangle = \sum_{i=1}^{N} T_i(\mathbf{k},\mathbf{k}'), \tag{5}$$

with N as the total number of sites. Let $T_i(\mathbf{k},\mathbf{k}') = \bar{T}(\mathbf{k},\mathbf{k}') + \delta T_i(\mathbf{k},\mathbf{k}')$, where $\bar{T}(\mathbf{k},\mathbf{k}')$ is the average of $T_i(\mathbf{k},\mathbf{k}')$ over the entire system, and $\delta T_i(\mathbf{k},\mathbf{k}')$ is the variation from the average. The average of the square of the scattering amplitude over the ensemble of configurations of the random alloy is then given by

$$\langle |T(\mathbf{k},\mathbf{k}')|^2\rangle = \sum_{i=1}^{N}\sum_{j=1}^{N} \langle \delta T_i^*(\mathbf{k},\mathbf{k}')\delta T_j(\mathbf{k},\mathbf{k}')\rangle, \tag{6}$$

in which we have used the assumption that the average $\bar{T}=0$. The quantity $\langle \delta T_i(\mathbf{k},\mathbf{k}')\delta T_j(\mathbf{k},\mathbf{k}')\rangle$ is the covariance between T_i and T_j, which vanishes unless $j=i$, since we have assumed that the contribution from different sites are statistically independent. As a result, the average of the square of the total scattering amplitude is

$$\langle |T(\mathbf{k},\mathbf{k}')|^2\rangle = \sum_{i=1}^{N} \langle |\delta T_i(\mathbf{k},\mathbf{k}')|^2\rangle = N\langle |\delta T_i(\mathbf{k},\mathbf{k}')|^2\rangle, \tag{7}$$

with $\langle |\delta T_i(\mathbf{k},\mathbf{k}')|^2\rangle$ as the variance of $T_i(\mathbf{k},\mathbf{k}')$, which is the same for all sites.

In SiGe, the sites are either occupied by Si or Ge, so that T_i is equal to $T_A = \langle \psi_{\mathbf{k}}|V_A|\phi_{\mathbf{k}'}\rangle$, with A=Si or Ge. The variance of this binary substitutional alloy can then be expressed in terms of the scattering produced by the substitution of an atom of one type for another:

$$\langle |\delta T_i(\mathbf{k},\mathbf{k}')|^2\rangle = x(1-x)|T_{\mathrm{Si}} - T_{\mathrm{Ge}}|^2. \tag{8}$$

Each site i in a SiGe alloy occupies a volume equal to $\frac{a_0^3}{8}$, that is, half of the volume of an fcc primitive cell, with a_0 as the lattice constant. The volume of the system is then $\Omega = N\frac{a_0^3}{8}$, and the scattering rate becomes

$$R(E(\mathbf{k}_\alpha)) = \frac{2\pi}{\hbar} x(1-x)\frac{a_0^3}{8}\sum_{\beta}\int \frac{d^3k'_\beta}{(2\pi)^3}|\langle V_{\alpha\beta}\rangle|^2 \times \delta(E(\mathbf{k}_\alpha) - E(\mathbf{k}'_\beta)), \tag{9}$$

where we have defined

$$\langle V_{\alpha\beta}\rangle = N(T_{\mathrm{Si}}^{\alpha\beta} - T_{\mathrm{Ge}}^{\alpha\beta}) = N\langle \psi_\alpha|V_{\mathrm{Si}}|\phi_\beta\rangle - N\langle \psi_\alpha|V_{\mathrm{Ge}}|\phi_\beta\rangle. \tag{10}$$

In the last equation we have removed the reference to the wave-vector $\mathbf{k}$, since the matrix elements do not depend strongly on them when $\mathbf{k}$ is in valley α and $\mathbf{k}'$ is in valley β. The reason for this is that the potential is short-ranged in comparison to the wavelength of the carriers. The potential V_A is that of a perturbation caused by the substitution of an atom of the periodic host by a type-A atom, and ϕ is the exact eigenstate in the presence of the perturbing potential that satisfies the boundary condition $\phi_{\mathbf{k}}(\mathbf{r}) \to \psi_{\mathbf{k}}(\mathbf{r})$, for $|\mathbf{r}|$ far away from the type-A atom. We can replace the integral over $\mathbf{k}'_\beta$ in Eq. (9) by one over the energy $E_\beta(\mathbf{k}')$, yielding

$$R(E) = \frac{2\pi}{\hbar} x(1-x)\frac{a_0^3}{8}\sum_{\beta}|\langle V_{\alpha\beta}\rangle|^2\rho_\beta(E), \tag{11}$$

where $\rho_\beta(E)$ is the density of states (DOS) per spin per unit volume in the final valley β at the carrier energy E. Both intravalley ($\beta=\alpha$) and intervalley ($\beta\neq\alpha$) terms are included in the total scattering rate.

The periodic host is represented in the VCA. We calculate the potential V_A by placing one A-type atom as a substitutional defect in a supercell of $N-1$ VCA host atoms. DFT is used to compute the single-particle electronic states $|\phi\rangle$ and to relax the atomic structure around the defect atom in the supercell. The CPA correction to the VCA band dispersion is calculated, and found to be small.[26]

Note that the use of the wave function ϕ is important in correctly calculating the scattering matrix element. The simpler form of first Born approximation, where ϕ is replaced by the undistorted Bloch wave function ψ, will not apply because the Si and Ge potentials are substantially different from the average host atomic potential near the ion and, as a result, the electronic wave function ϕ is quite different from ψ there. Moreover, the relaxation of the shells of atoms around the Si or Ge atom also distorts the wave function ϕ, compared with the Bloch state.

We use the ellipsoidal approximation in Eq. (1) to obtain the density of states per spin in valley β at the carrier energy E:

$$\rho^\beta(E) = \frac{\sqrt{m_l^\beta m_t^\beta}\sqrt{E-E_c^\beta}}{\sqrt{2}\pi^2\hbar^3}\Theta(E-E_c^\beta), \tag{12}$$

where $\Theta(a)$ is a unit step function (0 if $a<0$, 1 otherwise), E_c^β is the conduction band minimum energy, and m_l^β and m_t^β are the longitudinal and transverse effective masses, respectively, for valley β.

Two technical complications arise in finding the appropriate matrix element $\langle \psi_\alpha|\Delta V|\phi_\beta\rangle$ from a finite supercell: (a) The degenerate or nearly degenerate band states in the host supercell are mixed as a result of breaking the translational symmetry of the host by the A-type defect. Therefore, no eigenstate of the Hamiltonian satisfies the boundary condition $\phi_\beta(\mathbf{r}) = \psi_\beta(\mathbf{r})$ in the limit of $|\mathbf{r}|$ far away from the A-type atom. This problem is solved by defining a state as the linear combination of the nearly degenerate energy eigenstates $|\phi_i\rangle$ which has the largest overlap with the state $|\psi_\beta\rangle$, as explained in Ref. 10. (b) In a supercell, the zero of the potential is arbitrary and a physically well-defined way must be developed to compare the potential in the supercell with N host atoms and that with one type-A atom and $N-1$ host atoms.

A. Mixing of nearly degenerate states

The method for including the mixing of nearly degenerate states has been treated in Ref. 10. Here we present how to

obtain the scattering parameters directly from the band-structure calculations. It should be remarked that the choice of M in Eqs. (3) and (5) of Ref. 10 depends on the particular system under consideration, and is affected by the size of the supercell and by which bands fold into the Γ point in the Brillouin zone of the supercell. In our case, for instance, there is a range in composition where the Δ, L and Γ valleys cross, and are almost degenerate in energy, but well separated from other bands. Therefore, in the 64-atom supercell case, we consider $M=17$ to include the 6 X eigenstates, the 6 Δ-points, $\mathbf{k}=\frac{2\pi}{a_0}(\xi,0,0)$, etc., with $\xi=\frac{1}{2}$, the 4 L states, and 1 Γ state. The 128-atom supercell will require an $M=49$, since there are other bands folding into the Γ point with energies close to the conduction band minimum.

However, we should note that too big an M would recover the first Born approximation $|\phi_\beta\rangle=|\psi_\beta\rangle$. As we commented above, the correct state ϕ_β is distorted near the defect atom. This is not substantially altered by mixing the M low-lying conduction band states since each of these states will exhibit a similar distortion near the defect atom. However, if M is large enough to include all bands, then $|\phi_\beta\rangle$ in Eq. (3) of Ref. 10 becomes equal to $|\psi_\beta\rangle$.

Depending on the symmetry of the valley, the eigenvalues of the matrix in Eq. (4) of Ref. 10 will split in different ways. From these splittings we can obtain the inter- and intravalley scattering parameters for the Δ and L valleys. If we diagonalize the part of the matrix belonging to the Δ valley, the six originally degenerate eigenvalues split into threefold, twofold, and nondegenerate eigenvalues. From these, the scattering parameters can be obtained as follows:

$$V_\Delta = \frac{1}{6}(E_1 + 2E_2 + 3E_3), \tag{13}$$

$$V_{\Delta g} = \frac{1}{6}(E_1 + 2E_2 - 3E_3), \tag{14}$$

$$V_{\Delta f} = \frac{1}{6}(E_1 - E_2), \tag{15}$$

where E_i is the i-fold degenerate eigenvalue. Likewise, the four degenerate eigenvalues from the L valley split into a threefold and a nondegenerate eigenvalue. The scattering parameters are obtained from

$$V_L = \frac{1}{4}(E_1 + 3E_3), \tag{16}$$

$$V_{LL} = \frac{1}{4}(E_1 - E_3). \tag{17}$$

The parameters for the $\Delta - L$ scattering are obtained from the matrix elements between these two valleys, that is, from the elements in Eq. (4) of Ref. 10 in which α belongs to the Δ valley and β to the L valley, in the following way:

$$V_{\Delta L} = \sqrt{\frac{1}{24}\sum_{\alpha\in\Delta,\beta\in L} |\langle\psi_\alpha|dV^{\text{red}}|\psi_\beta\rangle|^2}. \tag{18}$$

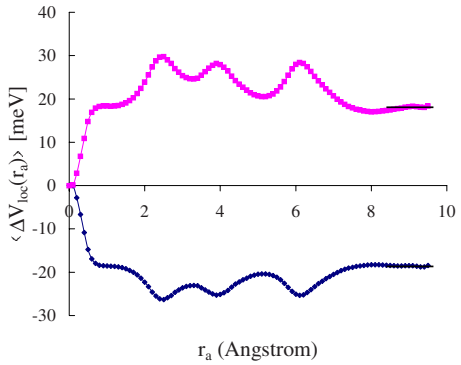


FIG. 2. (Color online) Averages of the potential difference [Eq. (19)] for distances greater than r_a from a Si atom (squares) or a Ge atom (diamonds) in a VCA ($x=0.5$) 64-atom supercell.

B. Potential zero shift

The expression for the scattering matrix $\mathbf{T}_i$ in Eq. (4) assumes that the perturbing potential V_i, due to the substitution of atom A at site i, tends to zero at large distance from site i. In a supercell calculation, the zero of potential energy is not physically well defined. In practice, the average of the local potential $V_{\text{loc}}(\mathbf{r})$ over the supercell is usually set to zero. However, in order to calculate properly the scattering T-matrix from Eq. (4), we must shift the zero of the local potential in the lattice containing a type-A atom, so that far from this atom it matches the corresponding potential in the periodic VCA host lattice.

To do this, we define the difference potential, $\Delta V^A_{\text{loc}}(\mathbf{r}_i) = V^A_{\text{loc}}(\mathbf{r}_i) - V^{\text{VCA}}_{\text{loc}}(\mathbf{r}_i)$, on the fast-Fourier-transform grid points $\mathbf{r}_i$ in an N-atom supercell. Here, $V^A_{\text{loc}}(\mathbf{r})$ is the local potential in the supercell containing one type-A atom (at the origin) and $N-1$ VCA atoms, and $V^{\text{VCA}}_{\text{loc}}(\mathbf{r})$ is the potential in a supercell of the same dimensions, containing N VCA atoms in a perfect diamond lattice. We then define the average potential difference at distances greater than r_a as

$$\langle\Delta V_{\text{loc}}(r_a)\rangle = \frac{1}{N_{\text{grid}}(r_a)}\sum_{i,|\mathbf{r}_i|>r_a} \Delta V^A_{\text{loc}}(\mathbf{r}_i), \tag{19}$$

where $N_{\text{grid}}(r_a)$ is the number of grid points for which $|\mathbf{r}_i| > r_a$ (Note that the distance $|\mathbf{r}_i|$, defined here, is the distance to the *nearest* image of atom A in the periodically repeated system defined by the supercell; alternatively, we assume that grid points $\mathbf{r}_i$ lie within the Wigner-Seitz cell for the supercell.). For supercells with 16 atoms or more, we find that $\langle\Delta V_{\text{loc}}(r_a)\rangle$ converges to a fairly constant value for large r_a, less than the Wigner-Seitz radius. This value is the required shift of the potential, to be subtracted from electronic eigenvalues for the system with one type-A atom, before the calculation of the reduced Hamiltonian in Eq. (5) of Ref. 10. Note that nonlocal parts of the atomic pseudopotentials are short-ranged and do not contribute to the average potential shift at large distance from atom A. Note also that the intervalley ($\alpha\neq\beta$) scattering parameters obtained in Eq. (4) of Ref. 10 from the reduced Hamiltonian, do not depend on the shift of the average potential in the supercell.

Figure 2 shows $\langle\Delta V_{\text{loc}}(r_a)\rangle$ as a function of r_a for a Si

atom or a Ge atom in a 64-atom supercell, where the VCA host has composition, $x=0.5$. By construction, $\langle \Delta V_{\mathrm{loc}}(r_a)\rangle = 0$ at $r_a=0$. All atomic positions have been relaxed in the supercell containing the Si (or Ge) atom to minimize the total energy of the system and the oscillations in $\langle \Delta V_{\mathrm{loc}}(r_a)\rangle$ for $r_a > 2$ Å are largely associated with the resulting relaxation of atoms from their ideal diamond lattice positions.

IV. INELASTIC SCATTERING BY PHONONS

A. Alloy phonon modes

In this section, we outline the methods used to calculate the phonon modes of the random alloy. We use density functional theory to calculate the forces in the alloy. The interatomic force constants in silicon and germanium are very similar and the differences in vibrational spectra arise principally from the difference in the atomic masses of silicon (m_{Si}) and germanium (m_{Ge}). (We will directly test this approximation for SiGe in Sec. VII A 2, below.) Following the approach of de Gironcoli and Baroni,[23] we will approximate the interatomic forces in the random alloy within the virtual crystal approximation. Using the random mass approximation, we then find the dynamical matrix of the alloy for an explicit random distribution of atomic masses.

We represent the short-wavelength and optical phonon spectrum and electron-phonon coupling in the alloy with that of a large supercell, containing N_s primitive diamond (fcc, two-atom) unit cells, with periodic boundary conditions. The supercell is a parallelepiped region, $\{\mathbf{r}=\eta_1\mathbf{A}_1+\eta_2\mathbf{A}_2+\eta_3\mathbf{A}_3 | 0\le\eta_i<1\}$, with sides defined by the vectors $\mathbf{A}_1$, $\mathbf{A}_2$, and $\mathbf{A}_3$. Germanium and silicon atoms are randomly distributed, each diamond lattice site being occupied by germanium, with probability x, or silicon, with probability $1-x$. In the fcc Brillouin zone, there are N_s wave vectors $\mathbf{q}$ that satisfy periodic boundary conditions on the supercell; i.e., $\exp[i\mathbf{q}\cdot\mathbf{A}_j]=1$, for $j=1,3$.

Thus, we calculate the interatomic force constants for the VCA periodic diamond structure, in which every atom has the ionic pseudopotential V_x^{VCA}, defined in Sec. II. For each wave vector $\mathbf{q}$, which satisfies periodic boundary conditions on the supercell, we calculate the 6×6 force constant matrix $\tilde{C}_{\tau,\alpha,\tau',\alpha'}(\mathbf{q})$ for the VCA diamond structure, where τ and τ' index the atom within the fcc unit cell ($\tau=1,2$) and α and α' label the Cartesian direction of motion ($\alpha=1,3$). This is calculated using the density functional perturbation theory method, as specified in Gonze and Lee.[27]

For an ordered diamond lattice, in which every atom has mass m, the eigenvalues of the dynamical matrix, $\mathbf{D}(\mathbf{q})=\tilde{\mathbf{C}}(\mathbf{q})/m$, are the square of the phonon frequencies $\omega_{\lambda,\mathbf{q}}$, $\lambda=1,6$, for momentum $\mathbf{q}$. The eigenvectors $u_{\tau,\alpha}(\lambda,\mathbf{q})$ of $\mathbf{D}(\mathbf{q})$ give the displacement $\mathbf{u}_\tau(\lambda,\mathbf{q})\exp[i\mathbf{q}\cdot\mathbf{R}]/\sqrt{m}$ of atom τ within the fcc unit cell at position $\mathbf{R}$ for the λ branch phonon mode of momentum $\mathbf{q}$. In an infinite, ordered diamond lattice, the interatomic force constants between atom τ in the unit cell at $\mathbf{R}_a$ and atom τ' in the unit cell at $\mathbf{R}_b$ are given by

$$\frac{\partial^2 E}{\partial r^a_{\tau,\alpha}\,\partial r^b_{\tau',\alpha'}} = C_{\tau,\alpha,\tau',\alpha'}(\mathbf{R}_b-\mathbf{R}_a) = \frac{V_{\mathrm{cell}}}{(2\pi)^3}\int_{\mathrm{BZ}} \tilde{C}_{\tau,\alpha,\tau',\alpha'}(\mathbf{q}) \times \exp[-i\mathbf{q}\cdot(\mathbf{R}_b-\mathbf{R}_a)]d^3\mathbf{q}, \tag{20}$$

where E is the total energy of the lattice, $\mathbf{r}^a_\tau$ is the displacement from equilibrium of atom τ in the unit cell at $\mathbf{R}_a$, V_{cell} is the volume of the diamond primitive unit cell, and the integral, $\int_{\mathrm{BZ}} d^3\mathbf{q}$, is over all wave vectors in the fcc Brillouin zone.

To find the vibration modes of the supercell, allowing for the explicit random distribution of silicon and germanium atoms, let us label the $2N_s$ atoms in the supercell with the index κ. For each atom, let $\mathbf{R}_\kappa$ be the position of the diamond unit cell in which it is located and τ_κ be its index within that cell. Thus, κ can be considered as a composite index $\{\tau_\kappa,\mathbf{R}_\kappa\}$ and summations over κ can be considered as a sum over the N_s values of $\mathbf{R}$ in the supercell and over $\tau=1,2$. The mass of atom κ is m_κ, which is the mass of either a silicon atom or a germanium atom. In the supercell with periodic boundary conditions, the interatomic force matrix is given by

$$C^{\mathrm{SC}}_{\kappa,\alpha,\kappa',\alpha'} = \frac{1}{N_s}\sum_{\mathbf{q}} \tilde{C}_{\tau_\kappa,\alpha,\tau_{\kappa'},\alpha'}(\mathbf{q})\exp[-i\mathbf{q}\cdot(\mathbf{R}_\kappa-\mathbf{R}_{\kappa'})], \tag{21}$$

where the summation $\Sigma_{\mathbf{q}}$ is over the N_s wave vectors $\mathbf{q}$ that satisfy periodic boundary conditions on the supercell. The dynamical matrix for the supercell with periodic boundary conditions is then

$$D^{\mathrm{SC}}_{\kappa,\alpha,\kappa',\alpha'} = \frac{1}{\sqrt{m_\kappa m_{\kappa'}}} C^{\mathrm{SC}}_{\kappa,\alpha,\kappa',\alpha'}. \tag{22}$$

Diagonalization of $\mathbf{D}^{\mathrm{SC}}$ yields eigenvalues ω_l^2 and normalized eigenvectors $u_{l,\kappa,\alpha}$, for $l=1,6N_s$. The vibrational frequencies of the supercell are ω_l and the displacement of atom κ in mode l is $\mathbf{u}_{l,\kappa}/\sqrt{m_\kappa}$.

For the very long-wavelength acoustic modes, the explicit distribution of silicon and germanium atoms has relatively little effect on the modes. In this limit, we can, not only treat the forces between atoms within the VCA, but also make the "average mass" approximation, viz. that each atom has a mass, $\bar{m}=xm_{\mathrm{Ge}}+(1-x)m_{\mathrm{Si}}$, equal to the average atomic mass in the alloy. Thus, the long-wavelength acoustic modes can be well represented by the corresponding modes of a perfect diamond lattice (without disorder) and intravalley electron scattering by acoustic phonons is well described within this picture of the alloy.

Due to the restriction of periodic boundary conditions on the supercell, the low-frequency, long-wavelength modes relevant for acoustic intravalley scattering are not well represented, even in supercells of several hundred atoms, which are quite adequate to represent the high-frequency phonon modes. For this reason, we calculate the acoustic intravalley scattering using the analytical approach of Herring and

Vogt,[6] which is based on the deformation potential model of coupling between electrons and long-wavelength acoustic modes. We calculate the deformation potential parameters from first principles, using a "frozen phonon" method (see Sec. IV C, below). In addition, this method allows us to directly verify the applicability of the deformation potential model for the phonon wave vectors relevant in intravalley carrier scattering.

B. Intervalley and optical phonon scattering

We now consider the scattering of carriers due to their coupling to the phonons of the alloy. The scattering rate due to absorption and emission of a phonon of energy $\hbar\omega_l$ is given by

$$R_{i\to f} = \frac{2\pi}{\hbar} \sum_{k,n,l,\pm} |\langle f|V_{\text{el-ph}}|i\rangle|^2 \delta(E_f - E_i), \tag{23}$$

where $\pm$ indicates sum over emission and absorption processes, $\langle f|V|i\rangle$ is the matrix element of the electron-phonon interaction between initial and final states, $|i\rangle = |n\mathbf{k}\rangle \otimes |n_l\rangle$ and $|f\rangle = |m\mathbf{k}'\rangle \otimes |n_l \pm 1\rangle$, respectively. Here, $|n\mathbf{k}\rangle$ is the Bloch electronic state of momentum $\mathbf{k}$ in band n for the VCA potential and $|n_l\rangle$ is the vibrational state of the alloy with n_l phonons in mode l. The energy of the initial state is

$$E_i = \epsilon_{n\mathbf{k}} + \sum_{l'} n_{l'} \hbar\omega_{l'} \tag{24}$$

and that of the final state is

$$E_f = \epsilon_{m\mathbf{k}'} + \sum_{l'} n_{l'} \hbar\omega_{l'} \pm \hbar\omega_l. \tag{25}$$

At temperature T, the average value of n_l is given by the Bose-Einstein distribution,

$$n_l = n(\hbar\omega_l) = (e^{\hbar\omega_l/k_B T} - 1)^{-1}, \tag{26}$$

where k_B is the Boltzmann constant. The electron-phonon interaction in the system of N_s diamond unit cells is[28]

$$V_{\text{el-ph}} = \sum_{l=1}^{6N_s} \sum_{\kappa=1}^{2N_s} \sqrt{\frac{\hbar}{2m_\kappa \omega_l}} \{a_l \mathbf{u}_{l,\kappa} + a_l^\dagger \mathbf{u}_{l,\kappa}^*\} \cdot \frac{\partial V_e}{\partial \mathbf{r}_\kappa}, \tag{27}$$

where a_l and $a_l^\dagger$ are the phonon destruction and creation operators, respectively, for mode l and $\frac{\partial V_e}{\partial \mathbf{r}_\kappa}$ is the derivative of the electronic potential with respect to the displacement of ion κ.

Electronic disorder is weak in SiGe and we calculate $\frac{\partial V_e}{\partial \mathbf{r}_\kappa}$ using the VCA for the ionic potential. Writing the composite index κ in the form $\{\tau, \mathbf{R}\}$, as defined in Sec. IV A, and bearing in mind that the electronic Bloch state $\psi_{n\mathbf{k}}(\mathbf{r})$, which is normalized in the supercell region of N_s diamond unit cells, satisfies the equation

$$\psi_{n\mathbf{k}}(\mathbf{r} + \mathbf{R}) = e^{i\mathbf{k}\cdot\mathbf{R}} \psi_{n\mathbf{k}}(\mathbf{r}), \tag{28}$$

the electronic matrix element can be written as

$$\langle m\mathbf{k}'|\frac{\partial V_e}{\partial \mathbf{r}_\kappa}|n\mathbf{k}\rangle = e^{-i(\mathbf{k}'-\mathbf{k})\cdot\mathbf{R}} \langle m\mathbf{k}'|\frac{\partial V_e}{\partial \mathbf{r}_{\tau,0}}|n\mathbf{k}\rangle = e^{-i\Delta\mathbf{k}\cdot\mathbf{R}} \frac{1}{N_s} \mathbf{H}^\tau_{\mathbf{k}'\mathbf{k}nm}, \tag{29}$$

where $\Delta\mathbf{k} \equiv \mathbf{k}' - \mathbf{k}$ is the change in momentum of the electron state in the scattering process. Here, $\mathbf{H}^\tau_{\mathbf{k}'\mathbf{k}nm}$ is a Cartesian vector, whose α component $H^{\tau\alpha}_{\mathbf{k}'\mathbf{k}nm}$ is the matrix element of the change in the potential due to the displacement of atom τ in direction α in the diamond unit cell at the origin, $\mathbf{R}=0$. This matrix element is the first-order Hamiltonian in Eq. (61) of Ref. 29, and can be obtained directly from density functional perturbation theory, using the VCA ionic potential.

The phonon absorption term (containing a_l) in the electron-phonon interaction can then be formulated as

$$\sqrt{\frac{\hbar}{2\omega_l}} \langle m\mathbf{k}'| \sum_{\kappa=1}^{2N_s} \frac{\mathbf{u}_{l,\kappa}}{\sqrt{m_\kappa}} \cdot \frac{\partial V}{\partial \mathbf{r}_\kappa} |n\mathbf{k}\rangle = \frac{1}{\sqrt{N_s}} \sqrt{\frac{\hbar}{2\bar{m}\omega_l}} \sum_{\tau=1}^{2} \tilde{\mathbf{X}}_{l\tau}(\Delta\mathbf{k}) \cdot \mathbf{H}^\tau_{\mathbf{k}'\mathbf{k}nm}, \tag{30}$$

where we have defined

$$\tilde{\mathbf{X}}_{l\tau}(\Delta\mathbf{k}) \equiv \sum_{\mathbf{R}} \sqrt{\frac{\bar{m}}{m_{\tau\mathbf{R}}}} \mathbf{u}_{l,\{\tau,\mathbf{R}\}} \frac{e^{-i\Delta\mathbf{k}\cdot\mathbf{R}}}{\sqrt{N_s}}, \tag{31}$$

with $\bar{m}$ as the average atomic mass, and $\mathbf{R}$ summed over the N_s primitive cells in the supercell. Notice that if there was no disorder and the phonon momentum $\mathbf{q}_l$ was well defined for each mode l, $\tilde{\mathbf{X}}_{l\tau}(\Delta\mathbf{k})=0$ unless $\Delta\mathbf{k}=\mathbf{q}_l$. In the disordered alloy, $\tilde{\mathbf{X}}_{l\tau}(\Delta\mathbf{k})$ gives the spatial Fourier transform of the atomic displacements of atom τ in the unit cell for phonon mode l. Defining

$$F^{\mathbf{k}'\mathbf{k}}_{m,n}(E) \equiv \sum_{l=1}^{6N_s} \left| \sum_{\tau=1}^{2} \tilde{\mathbf{X}}_{l\tau}(\mathbf{k}' - \mathbf{k}) \cdot \mathbf{H}^\tau_{\mathbf{k}'\mathbf{k}mn} \right|^2 \delta(E - \hbar\omega_l), \tag{32}$$

the carrier scattering rate from $|n\mathbf{k}\rangle$ into all $|m\mathbf{k}'\rangle$ by phonon absorption is

$$R^-_{n\mathbf{k}}(\epsilon_{n\mathbf{k}}) = \frac{2\pi}{N_s} \sum_{m,\mathbf{k}'} \frac{\hbar F^{\mathbf{k}',\mathbf{k}}_{m,n}(\epsilon_{m\mathbf{k}'} - \epsilon_{n\mathbf{k}})}{2\bar{m}(\epsilon_{m\mathbf{k}'} - \epsilon_{n\mathbf{k}})} \times n(\epsilon_{m\mathbf{k}'} - \epsilon_{n\mathbf{k}}) \Theta(\epsilon_{m\mathbf{k}'} - \epsilon_{n\mathbf{k}}), \tag{33}$$

where $\Theta(a)$ is a unit step function (0 if $a<0$, 1 otherwise). The scattering rate by phonon emission is

$$R^+_{n\mathbf{k}}(\epsilon_{n\mathbf{k}}) = \frac{2\pi}{N_s} \sum_{m,\mathbf{k}'} \frac{\hbar F^{\mathbf{k}'\mathbf{k}}_{m,n}(\epsilon_{n\mathbf{k}} - \epsilon_{m\mathbf{k}'})}{2\bar{m}(\epsilon_{n\mathbf{k}} - \epsilon_{m\mathbf{k}'})} \times [n(\epsilon_{n\mathbf{k}} - \epsilon_{m\mathbf{k}'}) + 1] \Theta(\epsilon_{n\mathbf{k}} - \epsilon_{m\mathbf{k}'}). \tag{34}$$

The total scattering rate is the sum of phonon absorption and emission rates:

$$R_{n\mathbf{k}}(\epsilon_{n\mathbf{k}}) = R^-_{n\mathbf{k}}(\epsilon_{n\mathbf{k}}) + R^+_{n\mathbf{k}}(\epsilon_{n\mathbf{k}}). \tag{35}$$

For optical and intervalley scattering, $F_{n,m}^{\mathbf{k}',\mathbf{k}}(E)$ has a weak dependence on $\mathbf{k}'$ and $\mathbf{k}$ near the conduction band valley minima, where the carriers are concentrated. Therefore, in calculating the optical phonon and intervalley scattering, we will approximate

$$F_{n,m}^{\mathbf{k}',\mathbf{k}}(E) \approx F^{\beta\alpha}(E), \tag{36}$$

where $\mathbf{k}$ is in the α valley of band n and $\mathbf{k}'$ is in the β valley of band m. Replacing $\frac{1}{N_s}\Sigma_k \rightarrow \frac{V_{\text{cell}}}{(2\pi)^3}\int d^3k$, where V_{cell} is the volume of a primitive diamond unit cell, and using the parabolic approximation given in Eq. (12) for the density of states in valley β, the scattering rate into valley β for carriers of energy E in valley α due to phonon absorption is

$$R_{\alpha\to\beta}^{-}(E) = \frac{V_{\text{cell}}\sqrt{(m_t^\beta)^2 m_l^\beta}}{\hbar^2\sqrt{2}\pi\bar{m}} \times \int_E^\infty dE' \frac{\sqrt{E'-E_c^\beta}F^{\beta\alpha}(E'-E)}{E'-E} n(E'-E). \tag{37}$$

Similarly, the scattering rate into valley β for carriers of energy E in valley α due to phonon emission is

$$R_{\alpha\to\beta}^{+}(E) = \frac{V_{\text{cell}}\sqrt{(m_t^\beta)^2 m_l^\beta}}{\hbar^2\sqrt{2}\pi\bar{m}} \times \int_{E_c^\beta}^E dE' \frac{\sqrt{E'-E_c^\beta}F^{\beta\alpha}(E-E')}{E-E'} [n(E-E')+1]. \tag{38}$$

C. Intravalley acoustic scattering

We calculate the acoustic phonon contribution to intravalley carrier scattering, following the deformation potential theory approach of Herring and Vogt,[6] as outlined in Fischetti and Laux.[1] In this section, we describe the calculation of the deformation potentials needed to compute the scattering of acoustic phonons in the Δ and L valleys, using a frozen phonon approach. We do not use the density functional perturbation theory approach of Ref. 27 because we find numerical instability in some of the parameters calculated, resulting in an extreme sensitivity to Brillouin zone sampling, for very long wavelength perturbations.

We need two deformation potentials for each valley in question: Ξ_d, the dilation deformation potential, and Ξ_u, the uniaxial deformation potential.[6] In the deformation potential approach, the effect of a long-wavelength acoustic phonon on the states in valley α is assumed to be equivalent to a slowly-varying potential,

$$V^\alpha(\mathbf{r}) = \Xi_d^\alpha Tr[\epsilon(\mathbf{r})] + \Xi_u^\alpha(\hat{\mathbf{k}}_\alpha \cdot \epsilon(\mathbf{r}) \cdot \hat{\mathbf{k}}_\alpha), \tag{39}$$

where $\epsilon(\mathbf{r})$ is the local strain tensor at $\mathbf{r}$ and $\hat{\mathbf{k}}_\alpha$ is a unit vector parallel to the $\mathbf{k}$-vector of valley α. The strain tensor is obtained by

TABLE II. Details of the frozen phonons used to calculate acoustic deformation potentials, Ξ_d and Ξ_u, for the Δ and L conduction band minima. The values of $C=\delta E/(q\delta R_0)$ from Eq. (43) for longitudinal and transverse phonons are given in columns three and four, respectively, in terms of the deformation potentials.

Valley	Direction of $\mathbf{q}$	Longitudinal	Transverse
Δ (010)	010	$\lvert\Xi_d+\Xi_u\rvert$	
Δ (001)	010	$\lvert\Xi_d\rvert$	
L (111)	010		$\lvert\frac{1}{3}\Xi_u\rvert$
	$0\bar{1}1$	$\lvert\Xi_d\rvert$	

$$\epsilon_{ij}(\mathbf{r}) = \frac{1}{2}\left(\frac{\partial\delta R_i}{\partial r_j} + \frac{\partial\delta R_j}{\partial r_i}\right), \tag{40}$$

where δR_i is the ith Cartesian component of the atomic displacement vector at $\mathbf{r}$.

For the Δ valley along the x direction, $\hat{\mathbf{k}}_\alpha=(100)$ and for the L valley along the [111] direction, $\hat{\mathbf{k}}_\alpha=(111)/\sqrt{3}$. Taking displacement of the atoms due to a phonon of momentum $\mathbf{q}$ and frequency ω as

$$\delta\mathbf{R}(\mathbf{r}) = \delta\mathbf{R}_0 \sin(\mathbf{q}\cdot\mathbf{r}-\omega t), \tag{41}$$

we find that the matrix element (at $t=0$) coupling electron states $|\mathbf{k}\rangle$ and $|\mathbf{k}'\rangle$, each in valley α, is

$$H_{\mathbf{k}'\mathbf{k}} = \langle\mathbf{k}'|V^\alpha(\mathbf{r})|\mathbf{k}\rangle = \frac{1}{2}\{\Xi_d\delta\mathbf{R}_0\cdot\mathbf{q} + \Xi_u(\hat{\mathbf{k}}_\alpha\cdot\delta\mathbf{R}_0)(\mathbf{q}\cdot\hat{\mathbf{k}}_\alpha)\} \times[\delta_{\mathbf{k}-\mathbf{k}',\mathbf{q}} + \delta_{\mathbf{k}'-\mathbf{k},\mathbf{q}}]. \tag{42}$$

For longitudinal phonons, we have $\delta\mathbf{R}_0 \| \mathbf{q}$, and for transverse phonons, $\delta\mathbf{R}_0 \perp \mathbf{q}$.

If the states, $|\mathbf{k}\rangle$ and $|\mathbf{k}+\mathbf{q}\rangle$, are degenerate in energy for $\delta\mathbf{R}_0=0$, then, for small $\delta\mathbf{R}_0$ and q, the phonon causes an energy splitting of these states,

$$\delta E = 2|H_{\mathbf{k}+\mathbf{q},\mathbf{k}}| = Cq\,\delta R_0, \tag{43}$$

where the constant C is determined by the phonon strain tensor and the acoustic deformation potentials. The sign of $H_{\mathbf{k}+\mathbf{q},\mathbf{k}}$ is obtained from the matrix element

$$M_{\mathbf{k},\mathbf{k}+\mathbf{q}} = \langle\mathbf{k}|\psi_+\rangle\langle\psi_+|\mathbf{k}+\mathbf{q}\rangle - \langle\mathbf{k}|\psi_-\rangle\langle\psi_-|\mathbf{k}+\mathbf{q}\rangle, \tag{44}$$

where $|\psi_+\rangle$ and $|\psi_-\rangle$ are the wave functions corresponding to the upper and lower eigenvalues resulting from the splitting due to the frozen phonon, respectively. In Table II, we give phonon directions and polarizations which allow us to calculate deformation potentials for the Δ and L valleys, along with the associated values of C in Eq. (43).

We calculate this splitting directly in DFT, using elongated supercells, as follows: We take phonon wave vectors $\mathbf{q}=\frac{4\pi}{Na_0}(0,1,0)$ along the [010] direction and $\mathbf{q}=\frac{4\pi}{Na_0}(0,-1,1)$ along the $[0\bar{1}1]$ direction, where N is an integer and a_0 is the cubic lattice constant. For $\mathbf{q}$ in the [010] direction, the transverse mode atomic displacement is in the [001] direc-

tion. For a given phonon wave vector $\mathbf{q}$, we choose the smallest supercell in which $\mathbf{q}$ is compatible with periodic boundary conditions. Defining the primitive diamond Bravais lattice basis vectors,

$$\mathbf{a}_1 = \left(0, \frac{1}{2}, \frac{1}{2}\right) a_0,$$

$$\mathbf{a}_2 = \left(\frac{1}{2}, 0, \frac{1}{2}\right) a_0,$$

$$\mathbf{a}_3 = (1,0,0) a_0, \tag{45}$$

we use a supercell with basis vectors, $\mathbf{A}_1 = N\mathbf{a}_1$, $\mathbf{A}_2 = \mathbf{a}_2$, $\mathbf{A}_3 = \mathbf{a}_3$, for the phonon with $\mathbf{q} = \frac{4\pi}{Na_0}(0,1,0)$ and a supercell with $\mathbf{A}_1 = \mathbf{a}_1$, $\mathbf{A}_2 = N\mathbf{a}_2$, $\mathbf{A}_3 = \mathbf{a}_3$ for $\mathbf{q} = \frac{4\pi}{Na_0}(0,-1,1)$. Atomic displacements specified by the acoustic phonon in Eq. (41) (for $t=0$) are made from the ideal diamond lattice positions within the supercell and the self-consistent DFT electronic potential is calculated. If $\mathbf{k}_\alpha$ is the Bloch momentum of the valley minimum, then we calculate the band energies in the supercell for Bloch momentum $\mathbf{k} = \mathbf{k}_\alpha - \mathbf{q}/2$ and find the splitting δE between the eigenstates, $[|\mathbf{k}_\alpha + \mathbf{q}/2\rangle + |\mathbf{k}_\alpha - \mathbf{q}/2\rangle]/\sqrt{2}$ and $[|\mathbf{k}_\alpha + \mathbf{q}/2\rangle - |\mathbf{k}_\alpha - \mathbf{q}/2\rangle]/\sqrt{2}$. In these calculations, we use the VCA potential V_x^{VCA} for all atoms in the supercell.

Since there are two atoms in the diamond unit cell (at equilibrium positions, $\mathbf{r}_\tau$, $\tau = 1,2$), then the pure acoustic displacement, $\mathbf{u}_{\tau\mathbf{R}}^{\mathrm{ac}} \equiv \sqrt{m}\,\delta\mathbf{R}_0 \sin[\mathbf{q}\cdot(\mathbf{R}+\mathbf{r}_\tau)]$, and the pure optical displacement, $\mathbf{u}_{\tau\mathbf{R}}^{\mathrm{opt}} \equiv (-1)^\tau \sqrt{m}\,\delta\mathbf{R}_0 \sin[\mathbf{q}\cdot(\mathbf{R}+\mathbf{r}_\tau)]$, are coupled for a general phonon wave vector and polarization, and the low-frequency (acoustic) vibrational mode is a mixture of both. Thus, in general we need to find the acoustic and optical components of the restoring forces on the atoms in the unit cell for both optical and acoustic frozen phonon displacements. Diagonalizing the resulting 2×2 dynamical matrix, we obtain the correct mixture of the optical and acoustic displacements in the acoustic mode (and in the optical mode).

We note that, for the high-symmetry phonons considered here, the phonons are either pure longitudinal or pure transverse, so that the full 6×6 dynamical matrix $\mathbf{D}(\mathbf{q})$ does not need to be solved. Moreover, for $\mathbf{q} \| [0\bar{1}1]$, the optical and acoustic displacements completely decouple by symmetry. The deformation potentials for the Δ valley are insensitive, by symmetry, to the mixture of optical displacements in the acoustic mode, but those of the L valley are quite sensitive. We note that an admixture of the optical mode in an infinite wavelength acoustic phonon is equivalent to a change in the equilibrium internal atomic displacement parameter for a strained crystal. The sensitivity of the L valley electronic levels to the internal atomic displacement parameter has been emphasized by Van de Walle and Martin.[7]

Deviations from the deformation potential approximation for short-wavelength acoustic phonons can be seen directly from the q-dependence of δE. For a given type of phonon, δE is linearly proportional to q for small q. For larger q, we will see deviations from linearity. The long-wavelength deformation potentials can be found from the linear term obtained in a polynomial fit of the calculated $\delta E/\delta R_0$ vs q.

Another method for obtaining Ξ_u from Eq. (39) is to strain a primitive cell so that previously degenerate valleys break their degeneracy. The difference in energy between the valleys is then proportional to Ξ_u. This method has been previously used by van de Walle and Martin[7] to obtain Ξ_u^Δ for Si and Ξ_u^L for Ge. Since Ξ_d can only be obtained from an absolute shift in band energies, the shift in potentials must be obtained using a supercell heterostructure with a strained region next to an unstrained one.

The calculation of the scattering rate is accomplished following Herring and Vogt:[6] using Eq. (39) to calculate the squared matrix element along symmetry directions of the phonon wave vector and interpolating these with spherical harmonics to obtain its angular dependence. The relaxation times (or scattering rates) are calculated, inserting our deformation potentials into Eqs. (49) and (50) of Ref. 6. Experimental values of the elastic constants for Si and Ge are used, linearly interpolated with respect to Ge composition x to obtain those of the alloy.

V. EXPRESSION FOR TOTAL MOBILITY

Finally, to calculate the total mobility due to all the scattering processes we apply a formula similar to that used in Ref. 1, derived from the Boltzmann transport equation in the relaxation time approximation:

$$\mu^\gamma = \frac{4}{9}\frac{eN_v^\gamma}{n^\gamma k_B T}\left(\frac{1}{m_l^\gamma} + \frac{2}{m_t^\gamma}\right) \times \int_{E_c^\gamma}^{\infty} dE e^{E_F - E/k_B T}(E - E_c^\gamma)\rho^\gamma(E)\tau^\gamma(E), \tag{46}$$

where $\tau^\gamma(E)$ is the sum of the different contributions to the scattering, namely, the alloy, intra- and intervalley and optical phonon scattering of a valley of type γ ($=\Delta$ or L),

$$\frac{1}{\tau} = \frac{1}{\tau_{\mathrm{ac}}} + R_{\mathrm{alloy}} + R_{\mathrm{intervalley}}, \tag{47}$$

τ_{ac} is the acoustic phonon relaxation time, and R_{alloy} and $R_{\mathrm{intervalley}}$ are the elastic alloy and phonon intervalley scattering rates, respectively. $N_v^\Delta = 6$ and $N_v^L = 4$ are the number of valleys in the Δ and L bands, ρ^γ is the electronic density of states, and n^γ is the density of carriers in all valleys of type γ,

$$n^\gamma = 2N_v^\gamma m_t^\gamma \sqrt{m_l^\gamma}\left(\frac{k_B T}{2\pi\hbar^2}\right)^{3/2} e^{E_F - E_c^\gamma/k_B T}, \tag{48}$$

where E_F is the Fermi energy.

Numerically, Eq. (46) does not have to be integrated up to infinity, thanks to the decaying exponential due to the Boltzmann distribution. $10\,k_B T$ represents a good upper limit of integration. The total mobility is obtained by summing over the bands as follows:

$$\mu = \sum_\gamma r_\gamma \mu^\gamma, \tag{49}$$

where

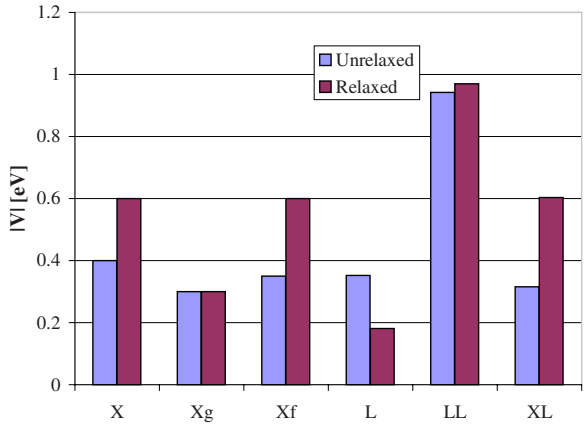


FIG. 3. (Color online) Calculated elastic alloy scattering parameters with relaxed and unrelaxed atomic positions around the perturbing atom (Ge), for the X and L points for pure silicon.

$$r_\gamma = \frac{n^\gamma}{n} \tag{50}$$

and $n=\Sigma_\gamma n^\gamma$ is the total carrier concentration.

VI. DETAILS OF ELECTRONIC STRUCTURE CALCULATIONS

Density functional theory total energy calculations are performed with the ABINIT code.[30,31] We use the local density approximation (LDA) for exchange and correlation. FHI pseudopotentials (available in the ABINIT website[31]) are used for all calculations in this paper. The calculation of the various parameters requires different cell sizes, k-point densities and energy cutoffs, which are described below. We use an energy cutoff of 18 hartree for the expansion of wave functions in all our calculations. The calculation of the electronic band dispersion has been performed as in Ref. 10.

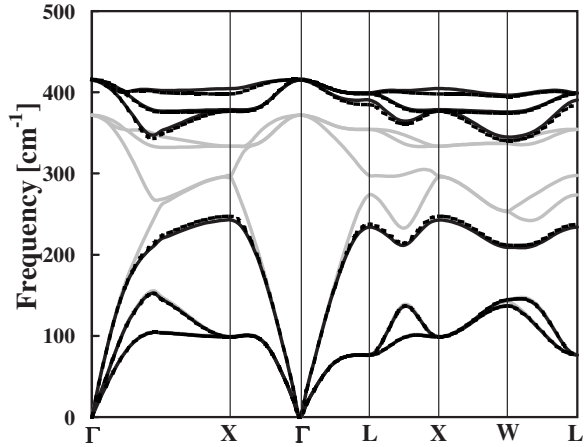


FIG. 4. Phonon dispersion for zincblende structure SiGe, calculated with full DFT (solid line), using VCA interatomic forces and correct Si and Ge atomic masses (dashed line), and using VCA interatomic forces and the average atomic mass of Si and Ge for both atoms (gray line).

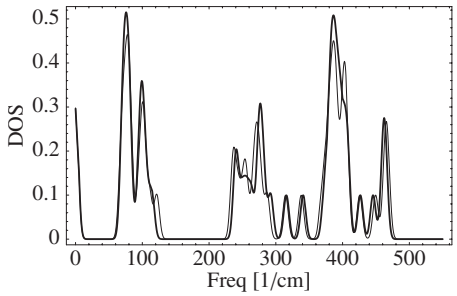


FIG. 5. Calculated phonon density of states for a 16-atom random alloy with composition $x=0.5$ using VCA forces and the random mass approximation (thick line), and using a full DFT calculation of the relaxed geometry and dynamical matrix (thin line).

A. Inelastic intervalley and optical scattering calculation

The intervalley and optical phonon scattering matrix elements $\mathbf{H}^{\tau}_{kk'nm}$ and the dynamical matrices are obtained in a diamond primitive unit cell, using the response function method,[29] available in the ABINIT code.[30,31] The modes and frequencies for the random alloy using random mass approximation are calculated in a 512-atom supercell with basis vectors,

$$\mathbf{A}_1 = 4a_0(1,0,0),$$

$$\mathbf{A}_2 = 4a_0(0,1,0),$$

$$\mathbf{A}_3 = 4a_0(0,0,1). \tag{51}$$

The phonon density of states is validated against a 1000-atom supercell, while all other calculations are performed using a 512-atom supercell. In calculating the function $F^{\beta\alpha}(E)$, the delta function in Eq. (32) is replaced with a finite-width Gaussian: $\delta(E-\hbar\omega_l) \rightarrow \exp[(E-\hbar\omega_l)^2/2\sigma^2]/\sqrt{2\pi\sigma^2}$, where $\sigma=3$ cm^{-1}, is chosen to be comparable to the typical separation between high-frequency mode frequencies ω_l in the finite supercell.

B. Frozen phonon calculation

In the frozen phonon calculations, we use the long supercells defined in Sec. IV C to obtain the energy splittings and

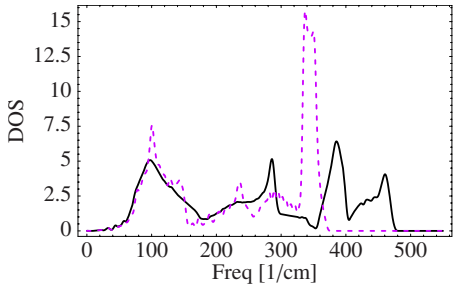


FIG. 6. (Color online) Calculated phonon density of states of $Si_{1-x}Ge_x$ at Ge composition $x=\frac{1}{2}$ for a disordered alloy, using the random mass approximation (solid line) and the average mass approximation (dashed line) in a 1000-atom supercell with periodic boundary conditions.

TABLE III. Calculated electron-phonon scattering matrix elements $H^{\tau,\alpha}_{\mathbf{k},\mathbf{k}'}$ (defined in Sec. IV B), with α as the Cartesian component, for the intervalley and optical scattering at the Δ and L valleys in $Si_{1-x}Ge_x$ as functions of alloy composition x. The intravalley optical phonon matrix element is labeled *opL*. Scattering by optical phonons with the Δ valleys is forbidden by symmetry. All quantities are in 10^9 eV/m.

Scattering phonon	$H^{\tau=1,\alpha=1}_{kk'}$	$H^{\tau=1,\alpha=2}_{kk'}$	$H^{\tau=1,\alpha=3}_{kk'}$	$\mathbf{H}^{\tau=2}_{kk'}$
Δg	0	0	$-22.734-4.598x+1.429x^2$	$\mathbf{H}^{\tau=1}_{\Delta g}e^{i\pi 3/4}$
Δf	$(-9.80348+0.48752x)i$	$-22.377-5.86x+1.88x^2$	$-H^{\alpha=1}_{\Delta f}$	$-(\mathbf{H}^{\tau=1}_{\Delta f})^*$
LL	$-2.09-5.746x+2.293x^2$	0	0	$\mathbf{H}^{\tau=1}_{LL}$
opL	$5.83+12x-3.05x^2$	$-H^{\alpha=1}_{opL}$	$-H^{\alpha=1}_{opL}$	$-\mathbf{H}^{\tau=1}_{opL}$
ΔL	$(-7.35-6.95i)+(0.31-4.73i)x-(0.05-1.26i)x^2$	$-H^{\alpha=1}_{\Delta L}$	$(-8.11+2.6i)-(1.78-3.62i)x+(0.26-0.75i)x^2$	$-(\mathbf{H}^{\tau=1}_{\Delta L})^*e^{-i\pi 5/8}$

wave functions due to phonon wave-vector $\mathbf{q}$ in different directions. We use supercells of $N=24$, 32, 48, and 64 atoms for the different lengths of $\mathbf{q}$, with a k-point grid of $6\times4\times6$. The amplitudes of atomic displacement defined in Eq. (41) we use are $|\delta\mathbf{R}_0|=1.25\times10^{-3}a_0$, $2.5\times10^{-3}a_0$, and $2.5\times10^{-2}a_0$, yielding a perfect linear dependence of $H_{\mathbf{k},k+q}$ on δR_0 within that range.

VII. RESULTS

A. Scattering parameters

1. Elastic scattering parameters

The elastic alloy scattering matrices have been calculated from first principles and have been given in Ref. 10. In this section we show that atomic relaxation near the Si or Ge atom in the supercell is found to have an important effect on the scattering factors; in some cases the scattering intensity is twice as large as that calculated keeping all atoms in their ideal diamond lattice positions, as can be seen in Fig. 3 for a Ge atom in a pure Si supercell.

2. Intervalley phonon scattering parameters

Figure 4 shows the phonon dispersion for zincblende $Si_{0.5}Ge_{0.5}$ calculated in various approximations. We see that the phonon dispersion calculated with VCA interatomic forces is extremely close to that found from a full LDA calculation. This result suggested the use of random mass approximation to calculate the phonon frequencies and modes in a random alloy. We also test the use of random mass approximation against a full calculation of a 16-atom random alloy, shown in Fig. 5. While there are some minor differences, the approximation yields good peak positions and intensities.

Figure 6 shows the density of states of a disordered $Si_{0.5}Ge_{0.5}$ alloy calculated using random mass approximation

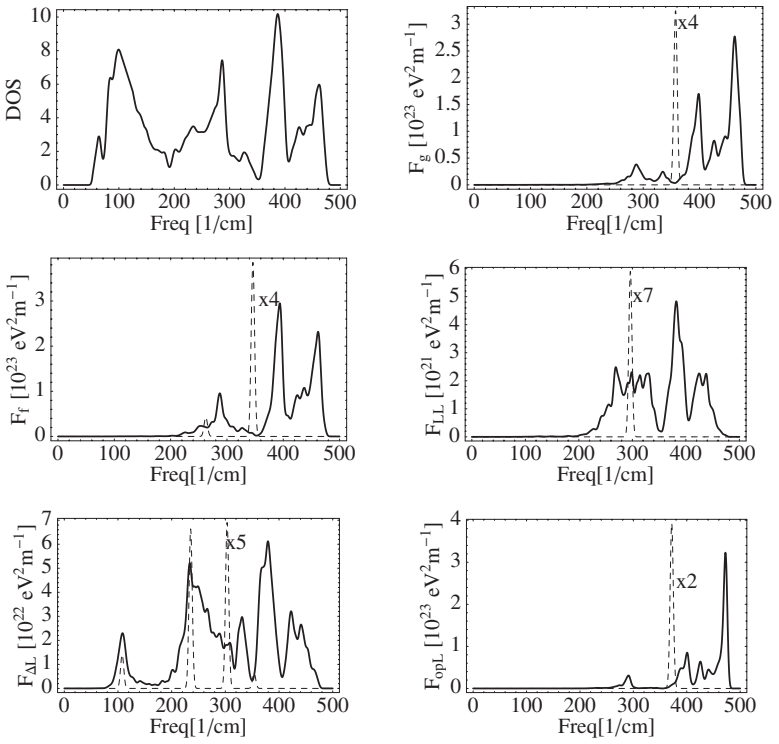


FIG. 7. Calculated density of states and F_{nm} functions for the different phonons: Δg, Δf, $L-L$, $\Delta-L$, and optical L using random mass approximation at Ge composition $x=0.5$. The values calculated using the average mass approximation are shown in dashed lines.

TABLE IV. Calculated deformation potentials at the Δ and L valleys in $Si_{1-x}Ge_x$ as functions of alloy composition x. All quantities are in eV.

Symbol	Function
$\Xi_{u\Delta}$	$4.2139x^3-6.7029x^2+3.4409x+8.7726$
$\Xi_{d\Delta}$	$-0.029-0.6642x$
Ξ_{uL}	$1.1733x^3-3.4080x^2+3.1747x+16.035$
Ξ_{dL}	$-2.6917x^3+3.8022x^2+0.1701x-7.5456$

in a 1000-atom supercell. The DOS of an alloy with an average mass $\bar{m}=xm_{\mathrm{Ge}}+(1-x)m_{\mathrm{Si}}$ is also shown. The disordered DOS compares well to previous calculations and experiment.[23] Notice that at very low frequencies the average mass density of states mimics that of the disordered supercell, justifying the argument presented in Sec. IV C for the use of an average mass to calculate the intravalley phonons.

We calculate the inelastic intervalley and optical phonon scattering rates from first principles for random alloys for Ge compositions of $x=0$, 0.25, 0.5, 0.75, and 1. The VCA electron-phonon matrix elements $\mathbf{H}^{\tau}_{kk'}$, are shown in Table III, as functions of x. To calculate the mobility, the intervalley scattering rates are interpolated in x for every value of energy E. Figure 7 shows the spectral resolution of the electron-phonon interaction $F(E)$ [(see Eq. (32)] for a Ge composition of $x=0.5$, with and without using random mass approximation. The inverse mobility shown in Fig. 9 is calculated using random mass approximation, but we should note that, using the average mass approximation, the contribution of the optical and intervalley scattering is reduced by only 6% in the mobility, which amounts to a 1% reduction in the total mobility at Ge composition $x=0.5$.

3. Intravalley phonon scattering parameters

We calculate the deformation potentials Ξ_u and Ξ_d from first principles with the method described above for the Δ and L valleys at Ge compositions of $x=0$, 0.25, 0.5, 0.75, and

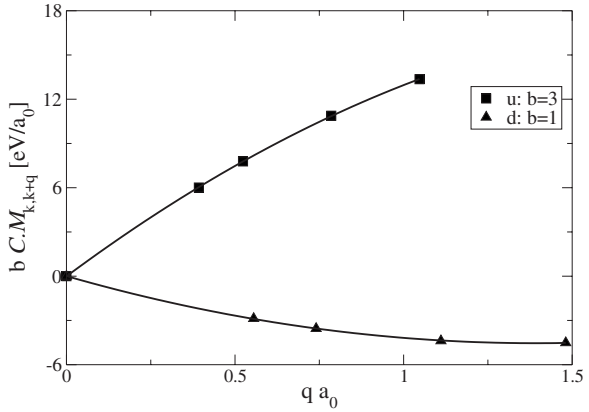


FIG. 8. Calculated phonon intravalley matrix element "d:" $C\cdot M_{\mathbf{k},\mathbf{k+q}}=\Xi_d|\mathbf{q}|$, and "$u$:" $3C\cdot M_{\mathbf{k},\mathbf{k+q}}=\Xi_u|\mathbf{q}|$ for the L valley in Ge as a function of phonon momentum $|\mathbf{q}|$, with q in the directions specified by Table II, interpolated with a polynomial fit. The linear term yields the deformation potentials [see Eq. (42)].

TABLE V. Deformation potentials for the conduction band extrema in Si and Ge. All values are in eV.

	Present work	Van de Walle[e]	Experiment
Ξ_u^{Δ}(Si)	8.77	9.16	8.6 ± 0.4 [a]
Ξ_d^{Δ}(Si)	−0.029	1.13	5[b]
Ξ_u^{L}(Si)	16	16.14	
Ξ_d^{L}(Si)	−7.55	−6.04	
Ξ_u^{Δ}(Ge)	9.73	9.42	
Ξ_d^{Δ}(Ge)	−0.67	−0.6	
Ξ_u^{L}(Ge)	16.98	15.13	16.2 ± 0.4 [c]
Ξ_d^{L}(Ge)	−6.27	−6.6	−12.3 [d]

[a]Reference 34.
[b]Reference 35.
[c]Reference 36.
[d]Reference 37.
[e]Reference 8.

1. Results are shown in Table IV, interpolated as functions of x. Table V compares our calculated deformation potentials with calculations by Van de Walle[8] and with experiment. Figure 8 shows the calculated $C\cdot M_{\mathbf{k},\mathbf{k+q}}$ from Eqs. (42) and (44) for different values of $\mathbf{q}$ in the directions specified in Table II for the L valley in pure Ge. The "d" line corresponds to a longitudinal phonon with $\mathbf{q}$ in the $[0\bar{1}1]$ direction. The line labeled "u" represents $3C\cdot M_{\mathbf{k},\mathbf{k+q}}$ for a transverse phonon with $\mathbf{q}$ along the [010] direction, for convenience. We can observe the deviations from the deformation potential approximation as q increases.

The intravalley phonon scattering rate is very important in determining the mobility in pure silicon or germanium, as can be inferred from Fig. 9. Equations (49) and (50) in Ref. 6 show the dependence of the scattering rate on the square of the deformation potentials Ξ_u and Ξ_d, as well as on their product. It is therefore crucial to calculate these as accurately as possible, since minor errors influence the mobility considerably.

B. Mobility

In Fig. 9 we present the contributions to the inverse mo-

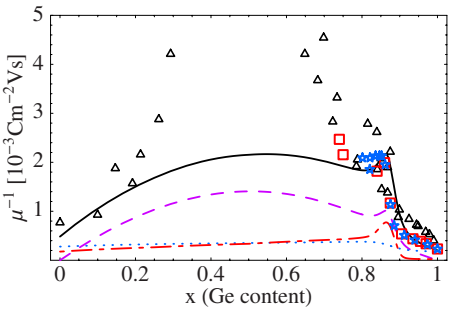


FIG. 9. (Color online) Calculated n-type inverse carrier mobility in $Si_{1-x}Ge_x$ at 300 K (solid line), inverse mobility due to acoustic phonon scattering only (dot), intervalley and optical phonon scattering (dashed-dotted line), alloy scattering (dashed), and experimental data from Refs. 32 (triangles), 17 (squares), and 33 (stars).

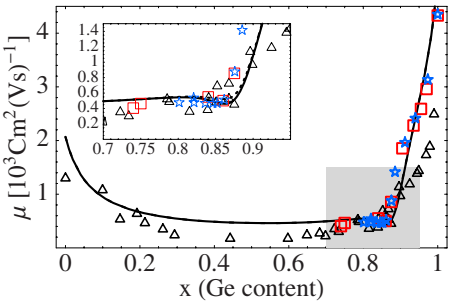


FIG. 10. (Color online) Calculated *n*-type carrier mobility in $Si_{1-x}Ge_x$ at 300 K (solid line), mobility without $\Delta-L$ alloy scattering (dash in inset), and experimental data from Refs. 32 (triangles), 17 (squares), and 33 (stars).

bility of the different scattering processes calculated from the Boltzmann transport equation in the relaxation time approximation (see Sec. V). It can be observed that the elastic alloy scattering is the most important contribution hampering the mobility for most of the range of compositions, except at pure Si or Ge, where acoustic scattering is of much greater significance. Acoustic phonon (intravalley) scattering dominates over intervalley and optical phonon scattering, except around the $\Delta-L$ valley crossover; here, where the two valleys are very close in energy, both the elastic and inelastic interband $\Delta-L$ scattering become important, as shown by the peaks at $x\sim0.85$.

Figure 10 shows the calculated total mobility as a function of alloy composition, compared to experiment. The agreement is excellent with Glicksmann[17] and Amith[33] who used single-crystalline samples, while the mobility is higher than that of Busch and Vogt,[32] as was expected since they used polycrystalline samples and did not subtract the ionized impurity scattering contribution.

VIII. CONCLUSION

We present the first full *ab initio* calculation, the disordered phonon *n*-type intervalley scattering parameters, and the acoustic deformation potentials for SiGe alloys as functions of alloy composition, using supercell methods to numerically represent the alloy scattering problem.

We find that, while disorder plays a crucial role in elastic alloy scattering, it does not affect the overall strength of the phonon scattering substantially, in spite of the loss of phonon momentum conservation. This result points out that, in spite of the fact that alloy disorder is essential in reproducing the three optical peaks in the phonon density of states, as found by de Gironcoli *et al.*,[23] an average mass model for the phonon structure is sufficient for obtaining the correct contributions of optical and intervalley phonon scattering to the carrier mobility.

We test the validity of the deformation potential approximation by calculating them at different phonon wave vectors, and find it to be good for scattering wave vectors dominant at room temperature. Optical and intervalley parameters, as well as the acoustic deformation potentials, are presented as functions of alloy composition in Tables III and IV, respectively.

We use our calculated scattering parameters in the Boltzmann transport equation to find the *n*-type mobility at room temperature. The resulting mobilities are in excellent agreement with experiment, in particular near the $\Delta-L$ band crossing region. The *ab initio* methods developed here are broadly applicable to a wide range of semiconductor alloys.

ACKNOWLEDGMENT

This work was supported by Science Foundation Ireland.

[1] M. Fischetti and S. Laux, J. Appl. Phys. **80**, 2234 (1996).
[2] D. J. Paul, Semicond. Sci. Technol. **19**, R75 (2004).
[3] L. Nordheim, Ann. Phys. **9**, 607 (1931); **9**, 641 (1931).
[4] R. J. Elliott, J. A. Krumhansl, and P. L. Leath, Rev. Mod. Phys. **46**, 465 (1974).
[5] J. W. Harrison and J. R. Hauser, Phys. Rev. B **13**, 5347 (1976).
[6] C. Herring and E. Vogt, Phys. Rev. **101**, 944 (1956).
[7] C. G. Van de Walle and R. M. Martin, Phys. Rev. B **34**, 5621 (1986).
[8] C. G. Van de Walle, Phys. Rev. B **39**, 1871 (1989).
[9] P. D. Yoder, V. Natoli, and R. M. Martin, J. Appl. Phys. **73**, 4378 (1993).
[10] F. Murphy-Armando and S. Fahy, Phys. Rev. Lett. **97**, 096606 (2006).
[11] S. Joyce, F. Murphy-Armando, and S. Fahy, Phys. Rev. B **75**, 155201 (2007).
[12] J. D. Sau and M. L. Cohen, Phys. Rev. B **75**, 045208 (2007).
[13] J. Sjakste, N. Vast, and V. Tyuterev, Phys. Rev. Lett. **99**, 236405 (2007).
[14] S. Krishnamurthy, A. Sher, and A.-B. Chen, Appl. Phys. Lett. **47**, 160 (1985).
[15] S. Krishnamurthy, A. Sher, and A.-B. Chen, Phys. Rev. B **33**, 1026 (1986).
[16] T. Manku and A. Nathan, IEEE Trans. Electron Devices **39**, 2082 (1992).
[17] M. Glicksman, Phys. Rev. **111**, 125 (1958).
[18] B. Pejcinovic, L. E. Kay, T.-W. Tang, and D. H. Navon, IEEE Trans. Electron Devices **36**, 2129 (1989).
[19] L. E. Kay and T.-W. Tang, J. Appl. Phys. **70**, 1483 (1991).
[20] M. S. Hybertsen and S. G. Louie, Phys. Rev. B **34**, 5390 (1986).
[21] K. J. Chang, S. Froyen, and M. L. Cohen, Solid State Commun. **50**, 105 (1984).
[22] X. Zhu, S. Fahy, and S. G. Louie, Phys. Rev. B **39**, 7840 (1989).
[23] S. de Gironcoli and S. Baroni, Phys. Rev. Lett. **69**, 1959 (1992).
[24] R. Dexter, H. Zeiger, and B. Lax, Phys. Rev. **104**, 637 (1956).
[25] F. Mandl, *Quantum Mechanics* (Butterworths, London, 1957).
[26] In the CPA there is a self-consistent determination of the self energy of the alloy, which is not done here. Since we find that the CPA corrections are small we do not expect them to have a

significant effect on the scattering rates.
[27] X. Gonze and C. Lee, Phys. Rev. B **55**, 10355 (1997).
[28] P. Yu and M. Cardona, *Fundamentals of Semiconductors* (Springer, Berlin, 2001).
[29] X. Gonze, Phys. Rev. B **55**, 10337 (1997).
[30] X. Gonze *et al.*, Comput. Mater. Sci. **25**, 478 (2002); http://www.abinit.org
[31] The ABINIT code is a common project of the Université Catholique de Louvain, Corning Incorporated, and other contributors (http://www.abinit.org).
[32] G. Busch and O. Vogt, Helv. Phys. Acta **33**, 437 (1960).
[33] A. Amith, Phys. Rev. **139**, A1624 (1965).
[34] L. Laude, F. Pollak, and M. Cardona, Phys. Rev. B **3**, 2623 (1971).
[35] A. Blacha, H. Prestind, and M. Cardona, Phys. Status Solidi B **126**, 11 (1984).
[36] I. Balslev, Phys. Rev. **143**, 636 (1966).
[37] D. Mirlin, V. Sapega, I. Karlik, and R. Katilius, Solid State Commun. **61**, 799 (1987).